Molecular Therapy
Methods & Clinical Development
Original Article

Inducible HEK293 AAV packaging cell lines expressing Rep proteins

Lovro Jalšić,[1,2] Viktoria Lytvyn,[2] Seyyed Mehdy Elahi,[2] Sabahudin Hrapovic,[3] Nasha Nassoury,[2] Parminder Singh Chahal,[2] Bruno Gaillet,[1] and Rénald Gilbert[1,2,4]

[1]Département de Génie Chimique, Université Laval, Québec, QC G1V0A6, Canada; [2]Department of Production Platforms and Analytics, Human Health Therapeutics Research Center, National Research Council Canada, Montréal, QC H4P 2R2, Canada; [3]Advanced Biomaterials and Chemical Synthesis Team, Aquatic and Crop Resource Development Research Centre, National Research Council Canada, Montréal, QC H4P 2R2, Canada; [4]Department of Bioengineering, McGill University, Montréal, QC H3A 0E9 Canada

Packaging or producer cell lines for scalable recombinant adeno-associated virus (rAAV) production have been notoriously difficult to create due in part to the cytostatic nature of the Rep proteins required for AAV production. The most difficult challenge being creating AAV packaging cell lines using HEK293 parental cells, currently the best mammalian platform for rAAV production due to the constitutive expression of *E1A* in HEK293 cells, a key *REP* transcription activator. Using suspension and serum-free media adapted HEK293SF carrying a gene expression regulation system induced by addition of cumate and coumermycin, we were able to create *REP*-expressing AAV packaging cells. This was achieved by carefully choosing two of the AAV Rep proteins (Rep 40 and 68), using two inducible promoters with different expression levels and integrating into the cells through lentiviral vector transduction. Three of our best clones produced rAAV titers comparable to titers obtained by standard triple plasmid transfection of their parental cells. These clones were stable for up to 7 weeks under continuous cultures condition. rAAV production from one clone was also validated at scale of 1 L in a wave bioreactor using serum-free suspension culture.

INTRODUCTION

Recombinant adeno-associated viruses (rAAV) are excellent vectors for *in vivo* gene therapy due to their wide tropism, absence of pathogenicity in humans, and long-term transgene expression stability without the need for genome integration.[1,2] The wild-type AAV genome consists of inverted terminal repeat (ITR) flanked *REP* and *CAP* genes that encode genome replication and packaging proteins as well as capsid proteins. rAAV vectors have *REP* and *CAP* replaced by a gene of interest making them replication defective with only ITRs remaining to enable replication and genome packaging. Therefore, the *REP* and *CAP* genes must be supplied separately from the rAAV genome for production.[3] *REP* promoters P5 and P19 generate Rep78 and Rep52 transcripts, which can be spliced to encode Rep68 and Rep40, respectively.[4–8]

Currently, transfection is the dominant method for rAAV production in HEK293 cells. rAAV production by transfection typically uses three plasmids that deliver *REP/CAP*, the rAAV genome, and adenoviral helper genes (*E2A, E4, VA-RNA*). In addition, the adenoviral helper genes *E1A* and *E1B* are integrated in HEK293 cells.[9] This triple plasmid rAAV production method is well suited for research and early clinical trials, but can be difficult to scale up due to issues emerging when performing large-scale transfection and high cost of materials.[10]

A drawback of rAAV vectors is the struggle of producing high-quality vectors in a scalable manner. Packaging cells containing some, or producer cells containing all genetic components for rAAV production offer a solution by reducing the amount or eliminating the need for plasmid in transfection. In addition, using producer cells would allow production at high cell density and increase volumetric production per batch due to the absence of transfection. In case of rAAVs, creating packaging or producer cell lines has proven difficult in the past due to the cytotoxic and cytostatic AAV and adenoviral components required for production.[11–16] Packaging cell lines that were described in scientific publications possess the drawback of using adenovirus co-infection during production instead of using a helper gene containing plasmid.[17–30]

Without helper gene expression, the complex regulation mechanisms of AAV promoters maintain tight transcriptional control.[31–34] For this reason, most described mammalian AAV packaging cell lines are HeLa,[17–24] or in some cases A549 cells,[25,26] which were not immortalized by adenovirus *E1A*, an activator of AAV *REP/CAP* transcription. Therefore, these cells are able to contain stably integrated endogenous *REP/CAP* and induced with adenovirus infection. While these cell lines allow easier creation of AAV packaging cells, the use of wild-type or replication defective adenovirus to deliver all helper functions also requires additional downstream processing to remove any residual adenovirus.[21,35]

Received 29 November 2022; accepted 11 July 2023;
https://doi.org/10.1016/j.omtm.2023.07.002.

Correspondence: Rénald Gilbert, National Research Council Canada, Building Montreal, 6100 Avenue Royalmount, Montreal, QC, Canada.
E-mail: renald.gilbert@cnrc-nrc.gc.ca

HEK293 cell lines are used for biomanufacturing recombinant protein and viral vectors due to their rapid growth rate, high transfectability, and adaptability to serum-free media and suspension culture.[36,37] Due to the constitutive expression of adenovirus *E1A* in HEK293 cells, the AAV P5 promoter becomes active, leading to Rep78 and Rep68 expression and cell-cycle arrest.[12,38,39] Reports of HEK293-based rAAV packaging cell lines are consequently few and use more elaborate approaches of *REP* expression regulation. The most notable examples are using Cre/*LoxP* recombination systems, but still using adenovirus infection.[27–29] Attempts using endogenous P5 or other constitutive promoters were shown to be challenging to isolate packaging cell lines and yielded unstable clones.[19,30]

The construction of an rAAV packaging cell line entails the stable integration of genetic elements necessary for the virus assembly (ITR flanked transgene, *REP*, *CAP*, and adenoviral helper genes) into permissive cells such as HEK293. Also, it is important that these genes are expressed at a sufficient level to obtain reasonable rAAV titers. Because of their toxicity, we consider the most difficult aspect of constructing such packaging cells to be the isolation of clones expressing *REP* in a stable manner at an adequate level. Therefore, we investigated if it was possible to isolate functional Rep clones utilizing inducible promoters in HEK293 cells. The induction system we used is based on a combination of the cumate[40] and coumermycin[41] inducible systems recently described for the development of lentiviral vector packaging cells.[42] Using this induction system, expression of Rep68 and Rep40 was sufficient to produce rAAVs. The characteristics of the rAAV produced using HEK293-Rep clones adapted to suspension culture and serum-free medium were comparable to the rAAV produced through the standard triple transfection method. In summary, this study describes a simple approach to generate HEK293 clones expressing Rep, one of the key elements to obtain packaging cells for rAAV.

RESULTS

Identification of Rep protein necessary for rAAV production in 293SF-CymR/λR-GyrB cells

Clear information on which combination of Rep protein is preferred for production, and if some of the more toxic Rep proteins can be omitted while maintaining a good titer is not available. To identify which of the four Rep proteins are necessary for rAAV production and investigate if there is a desirable combination yielding higher titers in 293SF-CymR/λR-GyrB cells, plasmids carrying the coding sequence of each individual Rep protein were constructed. The open reading frames (ORFs) of Rep proteins were designed to express only individual proteins by introducing mutations in the internal promoter p19 (TATTTAA to TACCTCT) for *REP78* and *REP68* and mutating the splice sites (CAGGTACCA to CCGCTACCA) for *REP78* and *REP52* while at the same time not affecting the amino acid sequence of Rep proteins. The expression of individual Rep proteins was verified with western blot (Figure 1A) of cells transfected with Rep ORFs expressed using the CMV (pCMV5-CuO) promoter. We assume the additional bands visible in the *REP2/CAP2* sample of Figure 1A are variable post-translational modifications of Rep protein specific to *REP2/CAP2* transfection. Similar patterns were observed in other publications.[43,44] These ORFs were also cloned into an expression cassette containing a CMV minimal core promoter, adenovirus tripartite leader sequence (Ad TPL), major late promoter (MLP) enhancer, and 12 copies of the lambda operator sequence (12xλ), which act as a binding site for the chimeric transactivator (λR-GyrB) of the coumermycin induction system.[41] The cells used for this study (293SF-CymR/λR-GyrB)[42] constitutively express the repressor protein of the cumate induction system (CymR) and conditionally express λR-GyrB using the cumate induction system. Transcription of λR-GyrB is controlled by the cumate inducible promoter CMV5CuO. CymR binds to the cumate operator (CuO) of the CMV5CuO promoter and represses transcription (Figure 1B). Addition of cumate dissociates CymR from CuO and permits transcription of λR-GyrB. In the presence of coumermycin, λR-GyrB dimerizes and binds to λOp to activate transcription (Figure 1C). Hence in this inducible system, transcription of the gene of interest is activated after addition of both cumate and coumermycin to the culture medium. The initial expression cassette used to express the individual Rep proteins under regulation of the cumate and coumermycin system was named pVR0 (Figure 1D).

To evaluate the production of rAAV using different combinations of Rep, we transiently transfected 293SF-CymR/λR-GyrB cells with a *CAP2* encoding plasmid (Figure 1G), gene of interest (GOI) (GFP)-ITR plasmid, plasmid encoding adenoviral helper genes, and combinations of pVR0-*REP* encoding plasmids and determined the produced functional titer (infectious viral particles per milliliter; IVP/mL) by transduction assay and flow cytometry. We compared the results with and without induction to rAAV production with the same cell line transfected with a *REP2/CAP2* plasmid, the same GOI (GFP)-ITR plasmid, and same helper plasmid (standard triple transfection method).

Production of rAAV (Figure 2A) was successful with all combinations except when no large Rep protein (Rep78 or Rep68) was used. The results obtained clearly show rAAV production in noninduced conditions at surprisingly high levels comparable to production by triple plasmid transfection with the standard *REP2/CAP2* plasmid. In induced conditions, Rep protein expression increased as expected (Figure S1). On the other hand, rAAV titer decreased in all cases, but not always significantly (Table S1). Titers obtained without induction using combinations of two, three, and all four Rep proteins, excluding the combination of Rep52 and Rep40, which does not produce AAV, showed no significant difference between each other. Using only one large Rep protein for production (Rep78 or Rep68) resulted in significantly lower production compared with other combinations.

Because of the highly cytostatic properties of Rep proteins,[11–14,16] leakiness of the expression system is undesirable for packaging cell line generation. To address if the observed expression level in the prior experiment is due to the nature of the inducible expression system, or high basal expression of the core promoter, we performed

Figure 1. Diagram of promoters used in the study and evidence for Rep expression

(A) Western blot image of Rep protein expression from *REP2/CAP2* plasmid (left image) and individual Rep expressed from the synthesized ORFs (right image) expressed from a pCMV5-CuO construct after transient transfection in HEK293SF cells. Western blot was performed with an antibody that binds to all four Rep proteins. (B) Diagram of expression system and Rep expression cassette in uninduced state. The CymR repressor binds to the CuO sequence and prevents transcription of the λR-GyrB transactivator and Rep68 in this example. (C) Diagram of expression system and Rep expression cassette in induced state. Addition of cumate releases CymR from the CuO sequence, which allows transcription of λR-GyrB. In the presence of coumermycin, λR-GyrB dimerizes and binds to the 12xλ operator and activates transcription of Rep68, in this example. (D) Inducible expression cassette (pVR0) used to identify necessary Rep proteins for AAV production. (E) Inducible Rep expression cassette pVR1 constructed for cell line generation. (F) Inducible Rep expression cassette pVR2 constructed for cell line generation. (G) Constitutive CMV driven AAV2 *CAP* expression cassette. Ad TPL, adenovirus tripartite leader; MLP enhancer, adenovirus major late promoter enhancer; CMV min, CMV minimal promoter.

rAAV productions with the same plasmid combinations in HEK293SF cells that do not produce the λR-GyrB transactivator and consequently do not possess the ability to activate transcription of the coumermycin inducible promoter.

The productions in HEK293SF cells (Figure 2B) using the same combinations of Rep-expressing plasmids yield similar titers of rAAV compared with 293SF-CymR/λR-GyrB cells, therefore confirming high basal expression of the core promoter.

As demonstrated by the previous experiments, rAAV production with different combinations of Rep protein is not significantly different regardless of using four, three, or two Rep proteins in HEK293SF and 293SF-CymR/λR-GyrB. Therefore, using only two for cell line generation would be more straightforward and would most likely facilitate isolation of viable clones. Since structural and functional research of Rep proteins was done in the past, the choice of minimally toxic protein according to the literature[11,12,45–61] with highest rAAV yields would be a combination of Rep68 with Rep40.

To create a stable cell line with inducible Rep expression, core promoter tightness is essential. Therefore, we modified the coumermycin promoter described in Figure 1D to minimize basal expression. In one version (pVR1, Figure 1E) the CMV minimal promoter was replaced by the TATA box sequence as core promoter while keeping the MLP enhancer and TPL sequence. In the second version (pVR2, Figure 1F), the MLP enhancer and TPL sequence were removed and the CMV minimal promoter was replaced by the TATA box sequence to have a minimal and tightly regulated expression cassette. Both cassettes contain 12xλ operator sequences upstream and a CuO sequence inserted downstream of the TATA box to prevent unwanted transcription in the absence of cumate and coumermycin by steric hindrance caused by CymR binding. Expression cassettes for Rep68 and Rep40 regulated with the pVR1 or pVR2 promoters were constructed (Figures 1E and 1F). The same pVR1 and pVR2 expression cassettes expressing GFP were also constructed for promoter characterization.

Promoter characterization in context of stable LV integration

To characterize the properties of the new promoters, we used the pVR1 GFP LVs and pVR2 GFP LVs to create stable cell lines in the same way as for the Rep packaging cell line. This would allow us to understand promoter tightness and expression profiles in context of stable LV integration. We created a pVR1-GFP and pVR2-GFP pool by transducing at MOI 5 and compared the levels of GFP expression by flow cytometry. The fluorescence indexes in Figure 3A show pVR1 expression cassette is 3-fold stronger than pVR2 in induced conditions demonstrating pVR1 provides higher expression than

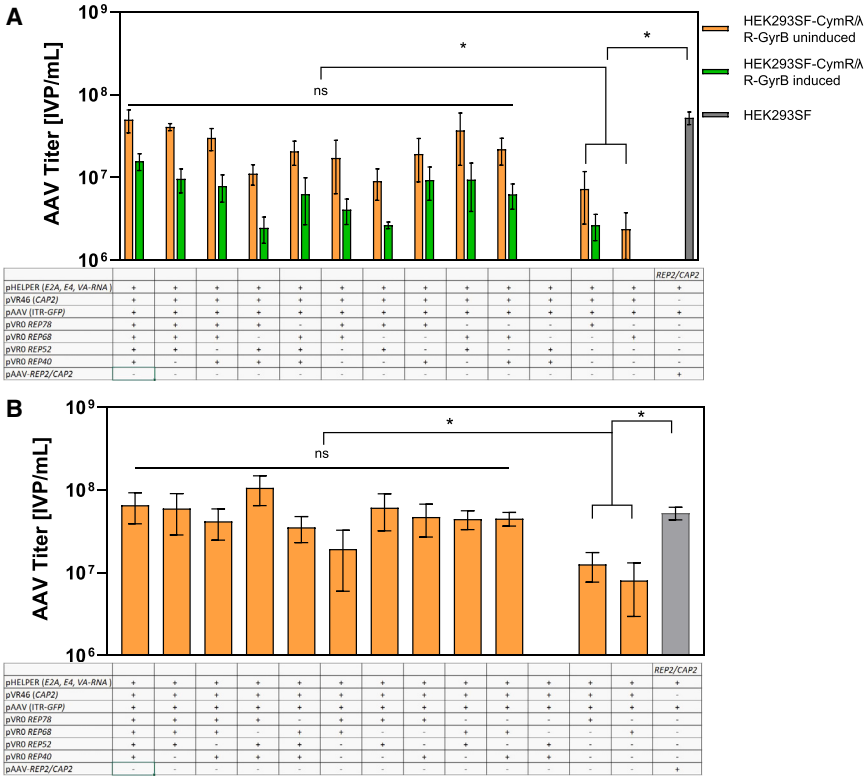

Figure 2. Identification of minimal Rep proteins for production of rAAV by transient transfection

(A) Functional rAAV titers obtained by transient transfection of 293SF-CymR/λR-GyrB cells with plasmids expressing Rep from inducible promoters. Brackets depicting significance refer to uninduced conditions only. (B) Functional rAAV titers obtained by transient transfection of HEK293SF cells with plasmids expressing Rep from inducible promoters, but without inducible expression system present in transfected cells (basal expression of core promoter). The data presented are infectious virus titers (IVP/mL) measured by flow cytometry 24 h after transduction of HEK293 cells. The table underneath the graphs contains information on combinations of plasmid used in transfection. Columns and error bars represent mean values and SD of n = 3 productions. Statistical significance is shown with * symbols (one and two * symbols represent $p \leq 0.05$, $p \leq 0.01$, respectively) and samples with no statistical significance are labeled with "ns".

pVR2. In uninduced conditions, pVR2 demonstrated higher promoter tightness as pVR1 is 7.7-fold stronger than pVR2.

We isolated 18 and 19 GFP-expressing clones transduced with pVR1 GFP LV and pVR2 GFP LV, respectively, from pools created using MOI 10. GFP expression level was monitored by flow cytometry in induced and uninduced conditions as well as different inducer concentrations. First, induced and uninduced conditions were monitored on pools and the isolated clones and then the selected clones were evaluated for the GFP expression levels at different inducer concentrations.

Clones transduced with pVR1 GFP LV showed measurable GFP expression in uninduced conditions, while pVR2 GFP LV transduced clones do not show detectable GFP expression in most analyzed clones. The mean of GFP-positive cells in uninduced conditions of all 18 analyzed pVR1 GFP clones was 88%. On the other hand, the mean of GFP-positive cells in uninduced conditions of all 19 analyzed pVR2 GFP clones was 6%. As a measurement of fold-induction, we observed the fluorescence index "on/off" ratio. The mean on/off ratio of pVR1 GFP clones was 5, while in pVR2 GFP clones it was 11,400 (Tables S2 and S3)

Out of 18 pVR1 GFP clones, all exhibited measurable GFP expression as demonstrated with example of an isolated clone in Figure 3B, while 11 of 19 pVR2 GFP clones did not show any detectable GFP expression in noninduced conditions ($\leq$0.1% GFP-positive cells) as in the example shown in Figure 3C.

Rep cell line generation and characterization

Our results demonstrated the tightness of the pVR2 promoter (Figure 1F) and higher expression level of pVR1 (Figure 1E) at the cost of promoter tightness. Since the main and most documented cytostatic and cytotoxic properties are from Rep68, the pVR2 promoter was used for its expression. The pVR1 promoter was selected for Rep40 expression since we assume better tolerance of cells to Rep40.

To create the Rep-expressing cell line, we transduced the 293SF-CymR/λR-GyrB cell line with *REP* encoding LVs. The MOIs of *REP68* and *REP40* used to create pools are listed in Table S4. From those two pools, clones were isolated and screened for rAAV production in 96 deep-well plates.

The rAAV-producing clones were expanded to six-well plates and tested for rAAV production for increased assurance in selection. Rep expression in the isolated clones during AAV production was confirmed with western blot and integrated *REP* gene copy number by droplet digital PCR (ddPCR) and additionally, we tracked expression levels and AAV productivity after a number of passages.

rAAV2 and AAV DJ production with isolated clones in six-well plate format and comparison to parental cell line

As clones D19 (from pool 1) and C8 and C24 (from pool 2) were identified as the best-producing clones, a comparison of functional rAAV titers produced in crude lysates was made with parental cell lines. The productions with parental cell lines (HEK293SF and

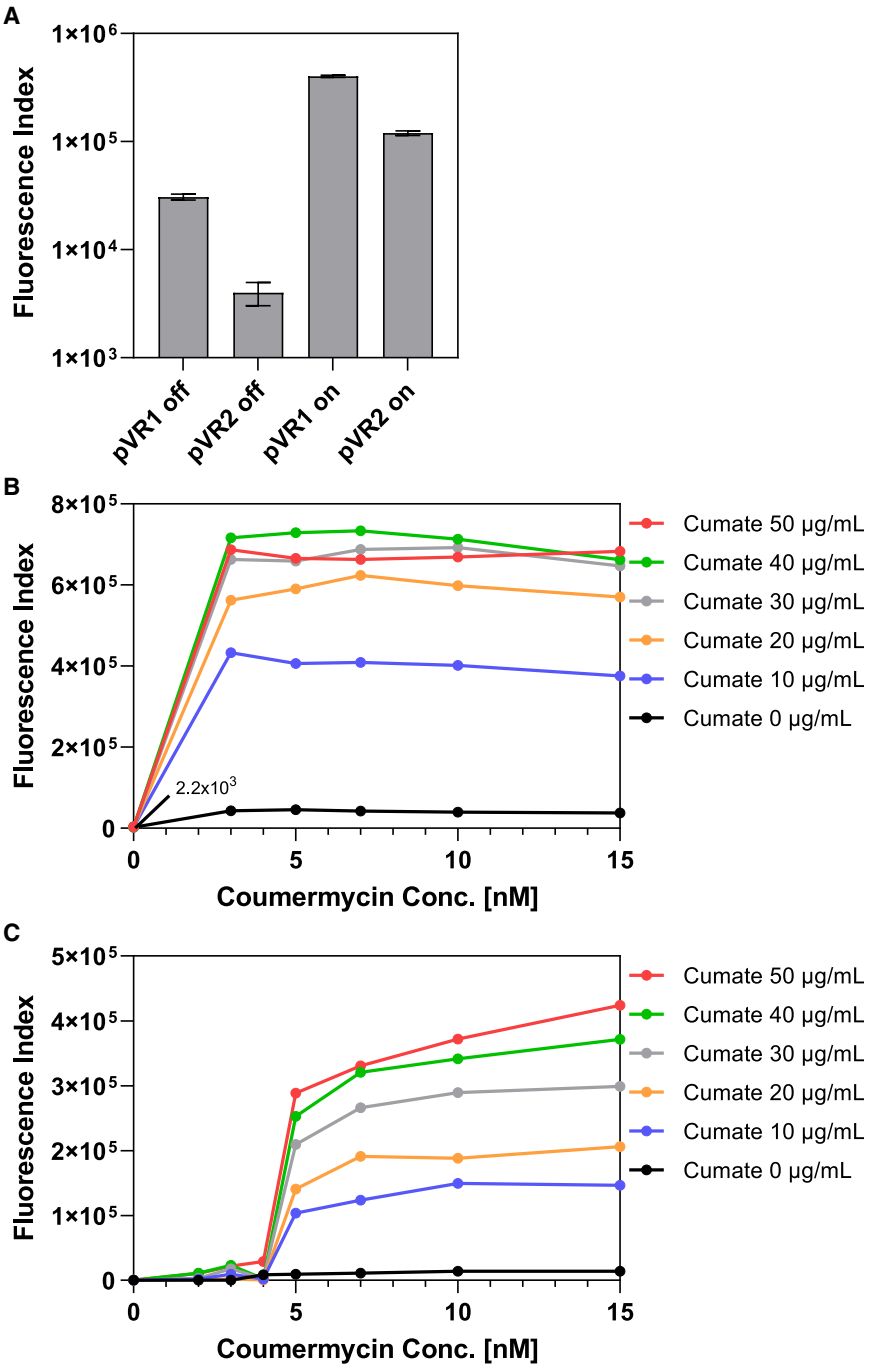

Figure 3. Comparison of pVR1 and pVR2 promoter activity in the context of lentivirus integration

(A) Fluorescence indexes of 293SF-CymR/λR-GyrB cells transduced with lentivirus containing pVR1 or pVR2 GFP expression cassette at MOI 5. Cells were analyzed 48 h after induction (72 h after transduction) by flow cytometry. Columns and error bars represent mean values and SD of n = 3 technical replicates. (B) pVR1 GFP-expressing clone induction profile at different inducer (cumate and coumermycin) concentrations. (C) pVR2 GFP-expressing clone induction profile at different inducer (cumate and coumermycin) concentrations. Cumate concentration (µg/mL) is indicated in the legend. Clones analyzed in (B) and (C) were obtained from a GFP pool created by lentiviral transduction at MOI 10 and isolated using the CelCelector robotic cell picking system. Cells were analyzed 48 h after induction by flow cytometry.

293SF-CymR/λR-GyrB) were done with standard triple plasmid transfection as well as five plasmid transfections containing plasmids encoding Rep expression cassettes used to create the stable cell lines (Figure 4A). We observed that functional titers produced by Rep-expressing clones were indistinguishable from each other, yielding about 3 × 10^7 IVP/mL in crude lysate. Comparison with standard triple plasmid transfection with *REP2/CAP2* plasmid showed no significant difference when parental 293SF-CymR/λR-GyrB cells are used, but compared with using HEK293SF cells, a statistically significant 1.7-fold difference was observed. Using 293SF-CymR/λR-GyrB cells to produce rAAV using Rep expression cassettes in uninduced conditions gave significantly lower titers (2.7-fold) compared with Rep clones, while induced conditions gave 3.4-fold lower titer compared with uninduced, similar to results presented in Figure 2A.

In addition to production of rAAV2, we also demonstrated the ability of the Rep clones to produce the chimeric (AAV2, 8, 9) rAAV DJ serotype (Figure 4B). The titers of rAAV DJ produced by Rep clones closely resemble those of rAAV2 (Figure 4A). There is no difference in rAAV DJ production when comparing the three Rep clones. Comparison of rAAV DJ production with HEK293SF and Rep clones reveals a statistically significant difference between Rep clone D19 and HEK293SF, but not when comparing C8 and C24 with HEK293SF.

In order to confirm our findings that the inducible GFP expression cassettes and induction (Figure 3) are valid for Rep expression and a plateau in induction is reached at inducer concentration of 30 µg/mL cumate and 10 nM coumermycin, we investigated the Rep expression and rAAV production at varying inducer concentrations with clone D19 (Figure S2). Our results confirmed no further increase in Rep expression or rAAV titer is achieved when the inducer concentration exceeds 30 µg/mL cumate and 10 nM coumermycin.

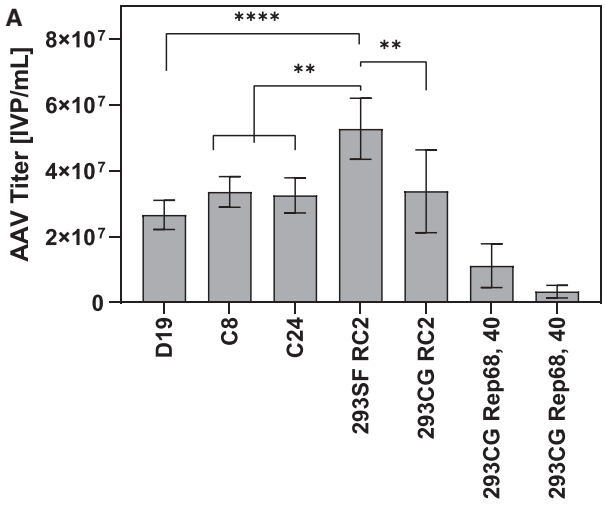

Figure 4. Functional rAAV titer of Rep-expressing clones and parental cell lines

(A) Production of rAAV2 serotype. Clones and cell lines were transfected with the indicated plasmids and AAV production was determined in the crude lysate at 72 h post transfection by flow cytometry. Columns and error bars represent mean values and SD of n = 5 to 7 productions. 293CG refers to 293SF-CymR/λR-GyrB cells. The data presented are infectious virus titers (IVP/mL) measured by flow cytometry 24 h after transduction of HEK293 cells. Statistical significance is shown with * symbols (two and four * symbols represent $p \leq 0.01$ and $p \leq 0.0001$, respectively). (B) Production of rAAV DJ serotype. Clones were transfected with pCMV-CAPDJ, pGFP-ITR, and pHelper and HEK293SF cells were transfected with pREP2/CAPDJ, pGFP-ITR, and pHelper. rAAV production was determined in the crude lysate at 72 h post transfection by flow cytometry. Columns and error bars represent mean values and SD of n = 3 productions. Statistical significance is shown with * symbol representing $p \leq 0.05$.

pHELPER (*E2A, E4, VA*-RNA)	+	+	+	+	+	+	+
pVR46 (*CAP2*)	+	+	+	-	-	+	+
pAAV (ITR-*GFP*)	+	+	+	+	+	+	+
pVR2 *REP68*	-	-	-	-	-	+	+
pVR1 *REP40*	-	-	-	-	-	+	+
pAAV-*REP2/CAP2*	-	-	-	+	+	-	-
Induction	+	+	+	-	-	-	+

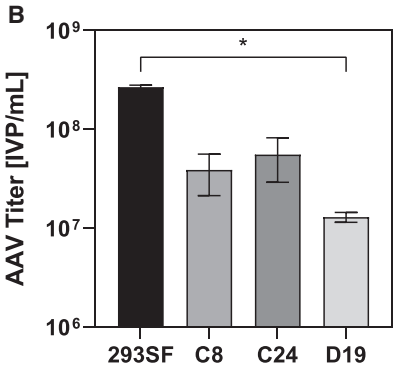

Comparison of Rep68 and Rep40 expression levels and AAV titers in the best-producing clones

We compared the levels of Rep68 and Rep40 at harvest (72 h post transfection) using semi-quantitative western blot. The relative levels of Rep68 and Rep40 expression in analyzed clones (Figure 5A) showed lower Rep68 expression in clone D19 compared with clones C8 and C24. The expression level of Rep68 was observed to always be lower than Rep40, as expected due to the difference in promoters. We also investigated the mRNA levels of the inducible *REP* genes with RT-ddPCR and using the housekeeping gene RPLP0 (Figure 5B). The induced condition demonstrates comparable patterns of expression to semi-quantitative western blot and uninduced conditions demonstrate the stringent Rep68 expression regulation using the pVR2 expression cassette.

While investigating the stability of AAV production and Rep expression, we found clones C8, C24, and D19 to be stable at least until passage 20 (1.5 months, Figure 6). The decrease in AAV production in later passages follows a decrease in Rep68, but not Rep40 expression, which remains at similar levels through all passages (Figures 6B and 6C).

Integrated *REP* copy number determination

The genomic DNA of Rep clones C8, C24, and D19 was isolated and ddPCR was performed to determine the *REP68* and *REP40* copy number (Table S5). The integrated copy number of *REP40* in analyzed clones is comparable to the MOI used to generate the original pool with varying numbers between different clones (between 6 and 12). The copy number of *REP68* on the other hand, was always lower than the MOI used and did not exceed three copies per cell in any analyzed clone. We also isolated the genomic DNA of the most promising clones after a number of passages to confirm constant *REP* copy number over time. In all tested clones, both *REP68* and *REP40* copy number did not significantly change at any point during culturing, with the exception of clone C8, where there is a significant difference between the *REP40* copy number between passages 5 and 24. In the case of clone D19, genomic DNA isolated at passage 36 after the observed decrease in titer showed no decrease in *REP68* or *REP40* copy number.

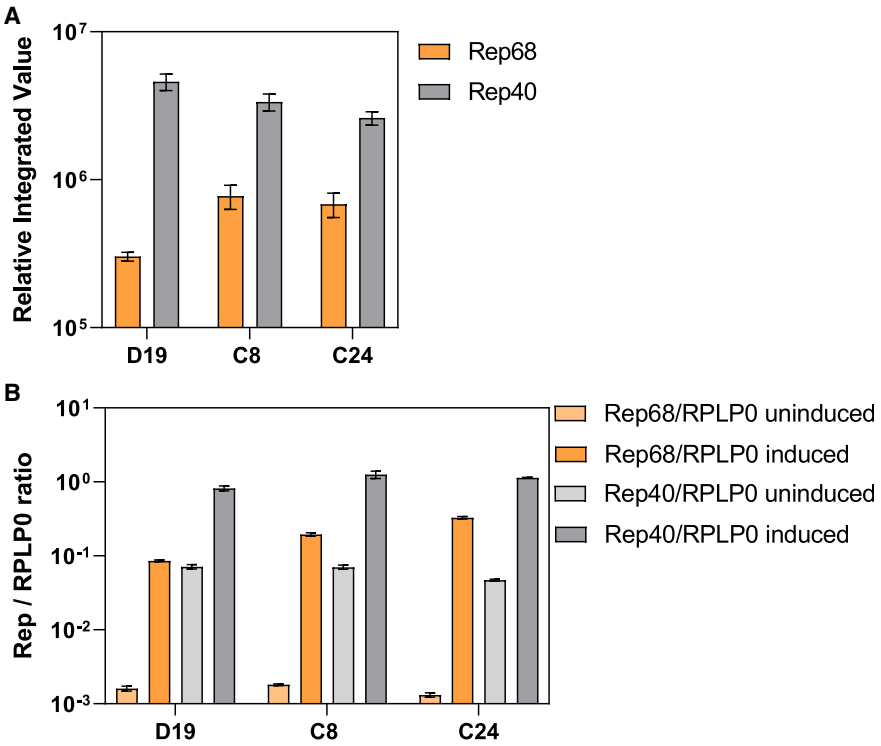

Figure 5. Relative expression level of Rep68 and Rep40 in stable Rep clones

(A) Expression levels analyzed by western blot at AAV harvest (72 h after induction), and normalization was done using total protein staining for loading normalization with TotalStain Q. (B) Rep mRNA levels measured by RT-ddPCR and normalized to housekeeping gene *RPLP0* expression level. Columns and error bars represent mean values and SD of n = 3 technical replicates.

AAV characterization

The rAAVs produced by the newly generated clones were titrated for their physical (ddPCR and total particle ELISA) and functional (transduction assay) titers. The material used for analysis was purified by iodixanol step gradient ultracentrifugation to remove residual reporter gene plasmid to avoid ddPCR titer overestimation.

The Rep-expressing packaging cells D19, C8, and C24 show no significant difference between them when comparing physical and functional titers (Figures 7A–7C). When comparing rAAVs produced with HEK293SF cells and Rep-expressing clones, no significant difference was observed in total particles produced. Although HEK293SF gives slightly higher functional and vector genome titer in shake flasks, rAAV production in wave bioreactor with D19 clone was comparable to HEK293SF cells for functional and vector genome titers. Comparing percentage of full capsids obtained from vector genome and total particle ratio (ddPCR/ELISA) shows 1.03%, 0.84%, and 0.82% genome-containing particles in clones D19, C8, and C24, respectively. Production with HEK293SF cells shows 14.33% genome-containing particles and wave bioreactor production using D19 clone shows 5.60% genome-containing particles. Transmission electron microscopy (TEM) of rAAVs produced using packaging cells (Figure 8) shows the same morphology as rAAV produced by triple plasmid transfection in HEK293SF cells.

DISCUSSION

In this study, we demonstrate the feasibility of generating high rAAV titer producing, inducible *REP*-expressing packaging HEK293 cell lines compatible with production using helper genes as opposed to adenovirus infection. We established that using Rep68 and Rep40, the least cytostatic Rep proteins,[11,12,45–61] yields titers comparable to other combinations of Rep protein, allowing us to have a simpler cell line generation method and higher probability of isolating rAAV-producing cells. Our method of pool generation using lentivirus, utilizing a robotic clonal cell picking system and screening in small volumes, allowed for gentler handling and faster generation of packaging cells compared with standard methods of stable transfection with antibiotic selection and limiting dilution. The MOIs of lentivirus used to create the cell lines were 10 or 15 for Rep68 encoding lentivirus and 10 for Rep40 encoding lentivirus (Table S4). While we attempted to isolate rAAV-producing clones from a lower MOI Rep68 pool (MOI 5), we were not successful. We have also attempted to generate clones where both Rep68 and Rep40 are expressed from the pVR2 expression cassette but were not successful and we believe

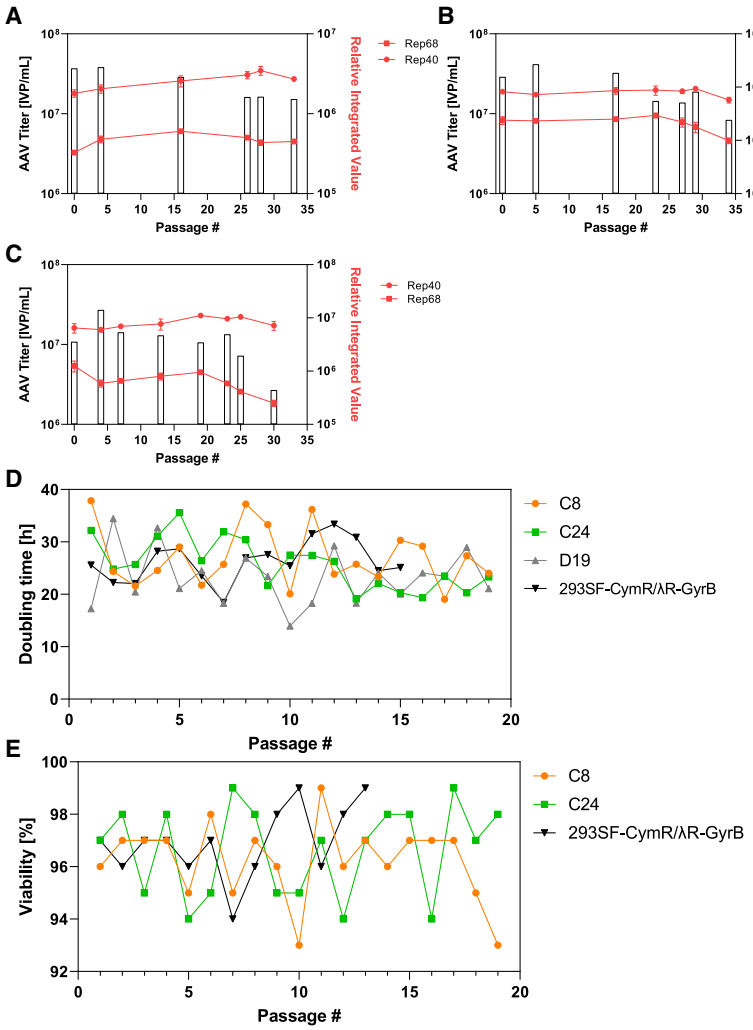

Figure 6. Stability study of Rep clones

Functional rAAV titer and Rep68 and Rep40 expression level over time (passages) in clones: (A) C8, (B) C24, (C) D19. (D) Doubling time of Rep-expressing clones and parental 293SF-CymR/λR-GyrB cells. (E) Viability of Rep cell line cultures. The rAAV titer data presented are infectious virus titers (IVP/mL) measured by flow cytometry 24 h after transduction of HEK293 cells. Expression levels analyzed by western blot at AAV harvest (72 h after induction), and normalization was done using total protein staining for loading normalization with TotalStain Q. The graph bars are the infectious virus particles (IVP) measured by flow cytometry after transduction of HEK293 cells. Lines represent Rep68 or Rep40 expression levels measured by semi-quantitative western blot where values and error bars are means and SD of n = 3 technical replicates.

in this case, Rep40 expression was not sufficiently high. The packaging cells we were able to isolate were able to produce titers comparable to rAAV production by triple plasmid transfection using the parental 293SF-CymR/λR-GyrB cells. In addition, we have demonstrated the stability of the packaging cells for at least 1.5 months in culture, a substantial problem for other HEK293-based packaging cells not utilizing a Cre/*LoxP* recombination system.[19,30]

The rAAV titer inhibition observed when Rep expression cassettes are induced in productions by transient transfection with 293SF-CymR/λR-GyrB cells (Figure 2A) is consistent with previous reports on rAAV titer inhibition by Rep overexpression.[62] Our data confirm previous studies that have indicated the minimal requirement of Rep78 or Rep68 and the inability of Rep52 and Rep40 to produce AAVs on their own.[63,64] In our case, after transient transfection rAAV production with Rep ORFs, we surprisingly obtained higher titer in uninduced conditions with most Rep ORFs. The particular level of expression achieved by using this configuration of coumermycin inducible promoter under uninduced conditions is shown to be beneficial for AAV production, but further expression after induction results in lower rAAV titers.

The rAAV productions by transient transfection (Figure 2B) demonstrate rAAV production in uninduced conditions is due to high basal core promoter transcription and not due to a leaky expression system. The HEK293SF cells used in this experiment do not possess the cumate and coumermycin expression system and the means to induce Rep expression, therefore only high basal expression of core promoters could cause the detected rAAV production. This observation is not surprising since the CMV minimal core promoter used is reported to have a relatively high basal expression compared with other core promoters.[65] In addition to the CMV minimal promoter, the other two promoter elements (MLP enhancer and TPL) in the construct most likely amplify the basal transcription, leading to a higher expression level in uninduced conditions.

Our choice of using a transduction assay for the initial experiments (Figure 2) and later screening of clonal cells is the convenience of analyzing a larger number of samples in a simple manner. Another reason is the difficulty of separation of transgene plasmid since nuclease is not sufficient to degrade the PEI-plasmid polyplexes, therefore making ddPCR or qPCR susceptible to titer inflation due to leftover plasmid found in unpurified lysate.

Investigating the promoters intended for Rep protein expression showed that the pVR2 (Figure 1F) promoter in pools has low basal GFP expression compared with the basal expression of pVR1 (Figure 1E). Additionally, when clonal cells were isolated from the pools, the 18 pVR1 GFP clones were all showing an average of

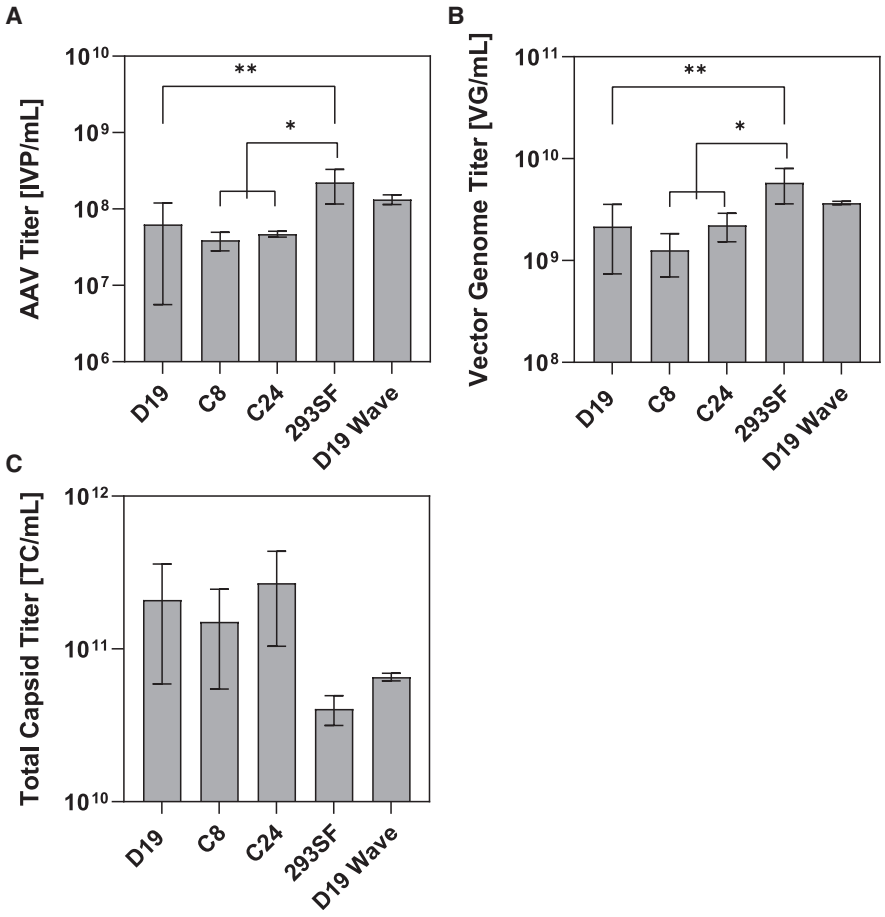

Figure 7. Comparison of functional and physical rAAV titer produced by Rep clones and HEK293SF cells

rAAV were obtained from 20 mL productions (D19, C8, C24, and HEK293SF) and a 1 L wave bioreactor production (D19 Wave). The material used for analysis was purified by iodixanol step gradient ultracentrifugation to remove residual reporter gene plasmid to avoid ddPCR titer overestimation. Rep clones and HEK293SF cells were transfected with a combination of plasmids indicated in Figure 4A. (A) Functional rAAV titer obtained from transduction assay (IVP/mL) measured by flow cytometry 24 h after transduction of HEK293 cells. (B) Vector genome titer (VG/mL, physical titer) obtained from ddPCR. (C) Total AAV capsid titer (TC/mL, physical titer) obtained from ELISA assay. Columns and error bars represent means and SD of n = 3 productions. Data of D19 1 L wave production are n = 3 technical replicates of one wave run. Statistical significance is shown with * symbols (one and two * symbols represent $p \leq 0.05$ and $p \leq 0.01$, respectively).

88% GFP-positive cells in culture in uninduced conditions (Tables S2 and S3). Further, the pVR2 GFP clones demonstrated that it is possible to isolate a clone with no detectable GFP expression when uninduced, a necessary feature for Rep68 expression regulation due to high toxicity. The induction profiles of pVR1 and pVR2 clones also demonstrate pVR1 is more sensitive at lower inducer concentrations than pVR2.

Functional rAAV titers obtained from lysates of Rep-expressing clones in six-well plates (Figure 4A) demonstrate the ability to produce rAAV vectors in the same amounts as parental 293SF-CymR/λR-GyrB or 1.5-fold lower than HEK293SF cells using the standard triple plasmid transfection production method. Interestingly, production of rAAVs using 293SF-CymR/λR-GyrB cells by five plasmid transfection where Rep68 and Rep40 are expressed from cassettes used to generate the isolated clones, yields a relatively high titer in uninduced conditions despite the minimal promoter used for *REP68* expression and no visible Rep68 band visible on western blot. The induced condition on the other hand still shows a decreased titer with clear visibility of both Rep proteins on western blot (Figure S3).

Productions of rAAV DJ, a chimeric serotype (AAV2, 8, 9)[66] achieved similar levels of rAAV production to AAV2, demonstrating the flexibility of the packaging system to produce serotypes other than AAV2 (Figure 4B).

Lower Rep68 expression in D19 compared with the other two clones is most likely due to D19 having one less gene copy than the other two clones. Despite the differences in copy number and expression level of both *REP68* and *REP40*, there is no observed difference in rAAV production between the clones. Furthermore, comparing titers obtained from initial transfection production using the same *REP68* and *REP40*

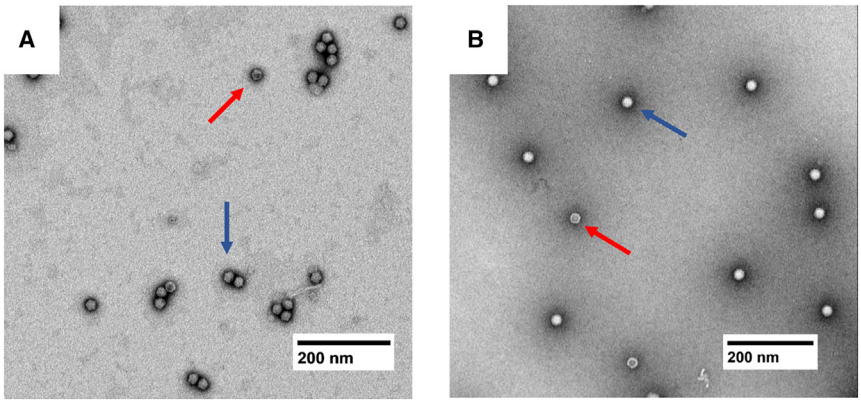

Figure 8. Comparative TEM analysis of rAAV produced in HEK293SF cells and Rep-expressing clones

AAV produced in HEK293SF cells (A) or D19 Rep clone (B) were purified by ultracentrifugation on iodixanol gradients and analyzed by TEM. Blue arrow points toward full rAAV capsid and red arrow points toward empty capsid.

expression cassettes (Figure 4A) with titers obtained from clones, shows that the clones exceeded the titer expectation.

The observed low integrated *REP68* copy number not matching the used lentivirus MOI could be explained with the toxicity of *REP68*.[11–14,16] As lentiviruses direct their integration into actively transcribed genes,[67] it is possible that the integration could occur downstream of a constitutive promoter and activate transcription of *REP68*, leading to cellular toxicity. Therefore, each *REP68* integration event presents a chance of constitutive expression occurring and resulting in cell-cycle inhibition and death of the clone, making it difficult to obtain higher *REP68* copy using lentiviral transduction. Another explanation could be that even though the expression cassette used is minimal, some expression still occurs, and cells could only tolerate the basal expression of a low copy number of *REP68*. While possible, this would most likely mean that isolated clones would be phenotypically distinct due to the basal expression, likely having a longer doubling time, yet the isolated clones show the same doubling time and viability as the parental cell line (Figures 6D and 6E).

Monitoring AAV production and Rep expression at later passages showed a decrease in *REP68* expression along titer decrease without changes in *REP40* expression. Since the *REP68* copy number is shown to be stable beyond the decrease in rAAV titer, an epigenetic silencing mechanism is likely to have caused a decrease of expression. The low integrated copy number of *REP68* makes it more vulnerable to epigenetic silencing as two or three loci are easily silenced to a point of affecting rAAV titer compared with the six or 12 copies as seen with *REP40*.

Before discussing titers obtained with the packaging cells, it is important to note that no production conditions were optimized for packaging cells except the concentration of inducer, which was shown to be optimal when full induction is achieved (data not shown). For production using HEK293SF cells, in-house optimized conditions specific to the cell line and triple plasmid transfection were used.[68] rAAV characterization revealed that isolated clones produce the same quantity and quality of vectors despite the observed differences in integrated *REP* gene copy number and expression levels.

The functional and vector genome titer produced by packaging cells, while being slightly lower than the production by triple plasmid transfection using parental HEK293SF cells (three and four times lower, respectively), could most likely be increased by optimizing the plasmid ratio (pCAP, pHelper, pAAV-GFP), production conditions, method, and possibly media. The wave bioreactor production with D19 clone demonstrated that the production method has an impact on titer and consequently reached functional and vector genome titer comparable to optimized HEK293SF triple plasmid transfection production. Although when we attempted to improve the percentage of genome-containing particles by using lower concentrations of pCMV-*CAP2* plasmid (Figure 1G) in transfection with Rep cell lines in small scale (six-well format), we did not see an improvement (data not shown). This would indicate the level of *CAP* expression is not the cause of high total particle production, but some other underlying factors with the system. Additionally, the wave bioreactor production using D19 clone showed lower total particle titer, further implying room for quality and titer increase with bioprocess optimization.

MATERIALS AND METHODS

Cell culture and AAV production

HEK293 cells adapted to serum-free suspension culture (clone 293SF-3F6) and HEK293SF-CymR/λR-GyrB cells are described elsewhere.[42,69] The AAV packaging cell lines were cultured in the same way as the parental HEK293SF-CymR/λR-GyrB cells.

Suspension cultures were maintained in 125 mL vented cap shake flasks (Corning, Oneonta, NY) in Hyclone Hycell TransFx-H (Hyclone, South Logan, UT) supplemented with 4 mM final concentration L-glutamine (Hyclone) and 0.1% final concentration kolliphor (Sigma-Aldrich, St Louis, MO) at 37°C, 120 rpm, and atmosphere with 5% CO_2. Static culturing used in cell line generation were maintained in a mixture (1:1) of Hyclone Hycell TransFx-H (Hyclone) supplemented with 4 mM final concentration L-glutamine (Hyclone) and 0.1% final concentration kolliphor (Sigma-Aldrich) and Hybridoma-SFM (Gibco, Life Technology Corporation Grand Island, NY) media supplemented with 4 mM final concentration L-glutamine (Hyclone), 10 ng/L transferin (Biogems, Westlake Village, CA), and 30 mM final concentration sodium bicarbonate.

The HEK293A cells (ATCC, Manassas, VA, Cat# CRL-1573) used for lentivirus titration were grown in Dulbecco's modified Eagle medium

(Hyclone) supplemented with 5% fetal bovine serum (Hyclone) and 2 mM final concentration L-glutamine (Hyclone) using tissue culture treated dishes.

Growth conditions for 96 deep-well plates (Corning) were 37°C, 950 rpm, and atmosphere with 5% CO_2 in Infors HT multitron 3-mm shaking throw incubator. Culture volume used was 300 μL.

Recombinant AAV production was performed in six-well plate in suspension format, with the exception of productions for screening (96 deep-well plate) and productions that were afterward used for ddPCR, electron microscopy, and ELISA (shake flask and wave bioreactor). Cell density at transfection was 1×10^6 cells/mL and media used Hyclone Hycell TransFx-H supplemented with 4 mM L-glutamine and 0.1% kolliphor unless indicated otherwise. Production incubation conditions were 37°C, 120 rpm, and atmosphere with 5% CO_2 unless indicated otherwise. Transfections were performed at final DNA concentration of 1 μg/mL and 2 μg/mL of PEIpro and transfection mixture was prepared in 5% of total cell culture volume with incubation time of 10–15 min.

Transfection for AAV production in 96 deep-well plates (Corning) was performed using final DNA concentration of 1 μg/mL and 2 μg/mL of PEI (PEIpro, Polyplus, Illkirch France). Cells were grown to approximately 2 million cells/mL density in 300 μL prior to transfection, 150 μL of culture was then removed. Transfection mixture was prepared in 5% of total cell culture volume with incubation time of 10–15 min, then added to 50% total culture volume of fresh media (150 μL). Then, 150 μL of plasmid/media mixture was added to the 150 μL cell culture in a deep-well plate resulting in a final cell density of 1 million cells/mL.

Cell culturing in the wave bioreactor system 20/50 (GE Healthcare, Uppsala, Sweden) for rAAV production using the D19 clone was performed by seeding cells in at 2.5×10^5 cells/mL in 500 mL media in a 5-L single use wave bioreactor bag (GE Healthcare, Uppsala, Sweden). The system was set to 37°C, 22 rpm at 8° angle, and 100 mL/min air flow. After 3 days, culture reached approximately 2×10^6 cells/mL and was diluted to 1×10^6 cells/mL in 1 L. Transfections were performed at final DNA concentration of 1 μg/mL and 2 μg/mL of PEIpro and transfection mixture was prepared in 5% of total cell culture volume with incubation time of 10–15 min. Inducer was added immediately after transfection at a final concentration of 30 μg/mL cumate and 10 nM coumermycin and angle was changed to 9.5°.

The concentrations of individual plasmids used in transfection are indicated in Table S6 in the supplementary information. The incubation of transfected cells lasted 3 days, except for the wave bioreactor production, which was 4 days, after which cells were lysed with $MgCl_2$ Triton X-100 and benzonase (EMD Millipore, Etobicoke, Canada) at final concentrations of 2 mM, 0.1%, and 2.5 U/mL, respectively. Lysis incubation lasted 2 h at previously described production conditions and $MgSO_4$ at final concentration of 37.5 mM was added and incubated for another 30 min. Lysis of samples for clone screening produced in 96 deep-well plate format was performed with three cycles of freeze-thaw.

Plasmids and cloning

Plasmids were constructed using standard methods of molecular biology. After amplification of plasmid in DH5α *E. coli*, purification was performed using commercial plasmid purification kits (Qiagen, Hilden, Germany). Concentration of plasmid or genomic DNA was measured using the Nanodrop spectrophotometer (Thermo Fisher Scientific, Waltham, MA).

The pAAV (ITR-GFP), pHelper, and pREP2/CAP2 are commercially available plasmids for rAAV production (Cell biolabs, San Diego, CA). The AAV2 *REP* ORFs (Rep78, Rep68, Rep52, Rep40) were synthetized and codon optimized for human cell expression (Genscript, Piscataway, NJ) (sequences provided in supplementary information, Figure S4). Mutations were introduced in the internal AAV p19 promoter (TATTTAA to TACCTCA) for *REP78* and *REP68* and the splice sites were mutated (CAGGTACCA to CCGCTACCA) for *REP78* and *REP52* while at the same time not affecting the amino acid sequence of Rep proteins. The ORFs of each individual *REP* were cloned into pUC57.

The pVR0 *REP* encoding plasmid depicted in Figure 1D was constructed as follows. The pVV 13xlambda-TPL VSVg Q96H-I57L plasmid described elsewhere[42] was cut with *BglII*/*NotI* to remove the *VSV-G* and inserting each synthetized *REP* open reading frame (*REP78, REP68, REP52, REP40*) using the same restriction enzymes.

The pVR1 and pVR2 expression cassettes were constructed by using plasmid pKCMV5-CuO (created by removing the Rev gene of pkCMV5CuO-Rev described elsewhere)[70] as template. The 12xλ-TATA box-CuO core promoter was synthesized (Genscript) and cloned into pUC57 using *SacI*/*XbaI* sites. For pVR1, the pKCMV5-CuO template was cut using *KpnI* and *AgeI* to remove the CMV5 promoter and CuO sequence and ligated with the 12xλ-TATA box-CuO core promoter cut using the same restriction enzymes. pVR2 was constructed by cutting the pKCMV5-CuO template with *Acc65I* and *BglII* to remove the CMV5 promoter, TPL, and MLP enhancer. The 12xλ-TATA box-CuO core promoter was ligated into the cut vector backbone using identical restriction sites.

pVR2-*REP68* was constructed by cutting pUC57-*REP68* with *EcoRI*/*StuI* and inserting the isolated cDNA in pVR2 *EcoRI*/*HincII* sites. pVR1-*REP40* was cloned using *BglII*/*SalI* sites in both pUC57-*REP40* and pVR1. The lentiviral transfer vector backbone pNRC-LV1 was described elsewhere.[42] pNRC-LV1-pVR2-*REP68* was cloned by cutting pVR2-*REP68* with *XhoI*, filling in the overhang and cutting with *NheI* while the pNRC-LV1 vector was cut with *HpaI*/*NheI*. pNRC-LV1-pVR1-*REP40* was cloned by cutting pVR1-*REP40* with *SmaI*/*NheI* and cutting pNRC-LV1 with *HpaI*/*NheI*.

The pCMV5-CuO-*REP* encoding plasmids used to express Rep in Figure 1A were constructed by cutting pUC57-*REP(78, 68, 52, 40)*

with *BglII/SalI* and inserting the isolated *REP* cDNA in pKCMV5-CuO (created by removing the Rev gene of pkCMV5CuO-Rev described elsewhere)[70] cut with *BglII/SalI*.

The pCMV-CAP2 plasmid was created by cloning of the CAP gene of AAV2 and its upstream untranslated region after the CMV5 promoter[71] of pTT3 (Patent WO2022147617A1).

The pCMV-CAP DJ plasmid was cloned by cutting of pAAV REP-CAP DJ (Cell biolabs) with NotI and HindIII and inserting into the pVV-CMV5 backbone that was cut using the same restriction enzymes. The pVV-CMV5 plasmid was constructed by removing a BglII/BbsI fragment containing the DS and FR sequence from the pTT5 vector,[72] filling in the ends and re-circularizing the plasmid.

Transduction assay for rAAV2 GFP

The procedure was described elsewhere and adapted for AAV transduction.[73] HEK293SF-3F6 cells used for the transduction assay were infected with first-generation adenovirus (Ad ΔE1, ΔE3) at MOI 5 and seeded at 0.5×10^6 cells/mL in suspension in 12-well plates (1 mL per well). Three dilutions of an AAV sample were prepared and 40 μL was added to the cells infected with adenovirus to ensure a range of GFP-positive cells of 2%–20% to ensure that cells were not transduced with more than one infectious viral particle. Positive control was an AAV sample with known titer and negative control was HEK293SF cells infected only with Ad (ΔE1, ΔE3). Infected cells were incubated for 24 h, transferred to deep-well plates (Corning) and pelleted by centrifugation for 2 min at 400 × *g*. Supernatant was removed and cells were resuspended in PBS with 2% formaldehyde. Fixed cells were read on a flow cytometer and percentage of GFP-positive cells was used to calculate the infectious viral particles titer (IVP/mL). The following formula was used to calculate titer:

$$IVP/mL = \frac{\%GFP\ sample - \%GFP\ negctl}{100} * Dilution\ Factor * \frac{\text{Average Cell Count}\left(\frac{\text{cells}}{\text{mL}}\right)}{40\mu L} * 1000\ \mu L/mL.$$

Generation of 293SF-Rep cells

We used lentivirus (LV) transduction for cell line generation to control the copy number introduced to cells by choosing different MOIs indicated in Table S3. Parental HEK293SF-CymR/λR-GyrB cells were plated in 24-well plates for growth in static conditions (1×10^5 to 2×10^5 cells/well). After 4 h or the next day when cells attached to the plate surface, media was removed and replaced with 500 μL media containing the appropriate concentration of Rep68 and Rep40 encoding LV with 8 μg/mL final concentration of polybrene (Hexadimethrine bromide; Sigma-Aldrich). Next day, media was removed from wells and fresh media was added. The pool was maintained for 3–7 days (until recovered from transduction) and plated for clonal cell picking using the CellCelector (ALS, Automated Lab Solutions GmbH, Jena, Germany). The clonal cell picking procedure is described elsewhere.[42]

AAV titration by ddPCR using EvaGreen DNA binding dye assay

AAV samples were serially diluted with 0.05% pluronic, 2 μg/mL sheared salmon sperm DNA. PCR reaction contained 0.1 μM of each primer, 0.4 mg/mL BSA, and 1x EvaGreen supermix (Bio-Rad Laboratories, Hercules, CA). Primers Fwd (5′-GGAACCCCTAGTGATGGAGTT-3′) and Rev (5′-CGGCCTCAGTGAGCGA-3′) used for AAV titration anneal to multiple sites within the ITRs and are described in detail elsewhere.[74] The following thermocycler setup was used: (1) Enzyme activation (95°C for 10 min); (2) 35 cycles of DNA denaturation (95°C 30 s), annealing (59°C 60 s), extension (72°C, 30 s); (3) signal stabilization (4°C, 5 min and 90°C, 5 min); and (4) infinite 12°C hold. The droplet generator (QX200), plate sealer (PX1), and droplet reader (QX200) used are made by Bio-Rad Laboratories and the thermocycler used was the Mastercycler X50s (Eppendorf, Hamburg, Germany).

Viral genomes per mL was calculated using the reported concentration of copies/μL and the following formula:

$$\frac{VG}{mL} = \frac{copies}{\mu L} * dilution\ factor * (20\mu L / 4\mu L) * 1000.$$

REP gene copy number determination by ddPCR using EvaGreen DNA binding dye assay

Genomic DNA was isolated using the Qiagen blood and tissue kit (Qiagen) according to manufacturer's recommendation. After isolation, 5 μg of genomic DNA was cut with 30 U of *MseI* restriction enzyme in 60 μL reaction volume for 2 h at 37°C. DNA was serially diluted with nuclease-free water. PCR reaction contained 0.1 μM of each primer, 0.4 mg/mL BSA, and 1x EvaGreen supermix (Bio-Rad Laboratories). Primers used for Rep68 expression cassette detection 55qF (5′-CAGATCCGGGAGAAGCTGAT-3′) and 55qR (5′-TGAGAGGTACTGCTCCATGTT-3′) amplify a 201-base pair (bp) sequence specific to *REP68*. Primers used for Rep40 expression cassette detection 56qF (5′- GCATGACTTCTGCGCTAAGAT-3′) and 56qR (5′- TCCTGGATCCACTGCTTCTC-3′) amplify a 217-bp sequence specific to the MLP enhancer used only in the Rep40 expression cassette and the 5′ end of the *REP40* sequence. Reference gene (Albumin) amplification was done using primers 57qF (5′-AGGCTAGGGCTTAGGGATTT-3′) and 57qR (5′-CCCTGTCCCACATGTACAAAG-3′) yielding a 56-bp fragment. The thermocycler setup used was the same as described for AAV titration.

The calculation of *REP* gene copies per cell was done using the ratio of *REP68* or *REP40* concentration and albumin concentration and multiplying by 3.2, which is the estimated albumin copy number in HEK293 cells[75]:

$$REP\ copies\ per\ cell\ =\ \frac{REP\ concentration\ [copies/mL]}{Alb\ concentration\ [copies/mL]} * 3.2.$$

RT-ddPCR for Rep68 and Rep40 mRNA quantification

mRNA was isolated from 4.5 million cells after 3 days of culturing (uninduced and induced conditions 30 μg/mL cumate and 10 nM coumermycin) using the RNeasy plus mini kit according to manufacturer recommendations (Qiagen). Reverse transcription was performed using QuantiTect kit (Qiagen) using 500 ng of RNA according to manufacturer recommendations (Qiagen). Primers used for Rep68 mRNA quantification 55qF (5′-CAGATCCGGGAGAAGCTGAT-3′) and 55qR (5′-TGAGAGG(PrimersATGTT-3′) amplify a 201-bp sequence specific to *REP68*. Primers used for Rep40 mRNA quantification 68qF (5′-TCCACTCCCAGGTCCAAAG-3′) and 56qR (5′- TCC TGGATCCACTGCTTCTC-3′) amplify a 94-bp sequence specific to the pVR1 expression cassette used for Rep40 expression and the 5′ end of the *REP40* sequence. The housekeeping reference gene used was *RPLP0* and primers were purchased as a set from IDT (Cat# Hs.PT.39a.22214824), sequences are: 5′-TCGTCTTTAAACCCTGC GTG-3′ and 5′-TGTCTGCTCCCACAATGAAAC-3′, PCR reaction contained 0.1 μM of each primer, 0.4 mg/mL BSA, and 1x EvaGreen supermix (Bio-Rad Laboratories). The following thermocycler setup was used: (1) enzyme activation (95°C for 10 min); (2) 35 cycles of DNA denaturation (95°C 30 s), annealing (59°C 60 s), extension (72°C, 30 s); (3) signal stabilization (4°C, 5 min and 90°C, 5 min); and (4) infinite 12°C hold. Droplet generator (QX200), plate sealer (PX1) and droplet reader (QX200) used are made by Bio-Rad Laboratories and the thermocycler used was Mastercycler X50s (Eppendorf).

Western blot and ELISA

Prior to rAAV harvest, 72 h post transfection, 1 mL of culture was centrifuged at 300 × *g* for 5 min. Supernatant was discarded and cell pellet was resuspended in PBS. Cells were again centrifuged at 300 × *g* for 5 min, supernatant was discarded, and cell pellet was lysed with 1x RIPA (0.25 mM Tris-HCl pH8.0, 150 mM NaCl, 5 mM EDTA, 0.1% SDS, 1% Triton X-100, 1% sodium deoxycholate) on ice for 30 min. Samples were sonicated and centrifuged for 20 min at 21,000 × *g* at 4°C and supernatant was then transferred into a clean tube on ice. Total protein quantification of samples was performed using DC protein assay (Bio-Rad Laboratories) according to manufacturer recommendation. Sample was prepared for loading on 4%–12% bis-tris Criterion (Bio-Rad Laboratories) polyacrylamide gel by mixing with XT sample buffer (Bio-Rad Laboratories) and DTT (50 mM) and incubating for 10 min at 70°C. SDS-PAGE was performed at 200 V for 30 min followed by transfer on nitrocellulose membrane using Trans-blot turbo transfer system (Bio-Rad Laboratories). Total protein staining for loading normalization was performed using TotalStain Q (Azure Biosystems, Dublin, CA, cat# AC2227) according to manufacturer recommendations. Membrane was incubated for 1 h in blocking buffer (1x PBS, 0.1% Tween 20 with 5% non-fat dry milk) followed by overnight incubation with 1:200 diluted primary antibody (Anti-Rep mouse monoclonal antibody, cat# 03–61069; American Research Products, Waltham, MA) at 4°C. Membrane was washed three times for 10 min on orbital shaker with washing buffer (1x PBS, 0.1% Tween 20) and incubated with fluorescent secondary antibody 1:10,000 dilution, goat anti-mouse immunoglobulin (Ig)G H&L IRDye 800CW (cat# ab216772; Abcam, Waltham, MA) for 1 h in blocking buffer. The membrane was then washed three times for 10 min on an orbital shaker with washing buffer and visualized on the imaging system Azure 600 (Azure Biosystems). Images for semi-quantitative western blot were analyzed using Azure Spot software (Azure Biosystems).

In the case of Figures 1E, S1, and S3, secondary antibody used was horseradish peroxidase-conjugated sheep anti-mouse IgG antibody (GE Healthcare, Backinghamshire, UK). The signal was revealed by chemiluminescence using the ECL western blotting detection reagents (PerkinElmer Inc., Boston, MA) and visualized with the Image Quant LAS 4000 mini biomolecular imager (GE Healthcare, Backinghamshire UK).

Total rAAV particle titer was determined using AAV2 Titration ELISA 2.0R kit (cat# PRAAV2R; Progen, Heidelberg, Germany) according to manufacturer recommendation.

GFP expression experiments for inducible promoter characterization

Promoter characterization in pools generated using LV transduction were performed in static conditions in 96-well plates. 293SF-CymR/λR-GyrB cells were plated (20,000 cells/well) and 4 h after plating when attached, transduction with LV was performed at MOI 5 as described above. After 24 h, inducer was added to the culture at final concentration of 80 μg/mL cumate 10 nM coumermycin. Forty-eight hours after induction (72 h after transduction), cells were fixed by adding formaldehyde to a final concentration of 2% analyzed by flow cytometry.

Expression level experiments using GFP clones were performed in suspension culture 24-well plates at 160 rpm shaking speed with addition of variable inducer concentration (cumate, coumermycin).

Electron microscopy

Observation by TEM (HITACHI H-7500, Japan) equipped with bottom-mounted AMT NanoSprint 12 MP camera and operating at 80 kV in high-contrast mode, was performed using a negative-staining technique. TEM grids (Cu 200 mesh, 15–25 nm carbon supported, Ted Pella Inc.) were freshly glow-discharged using EMS GloQube-D, dual chamber glow discharge system (Electron Microscopy Sciences, PA) in negative mode with plasma current of 25 mA for 45 s. Such grids were floated on 10 μL AAV aliquots on the Parafilm for 3 min. The excess droplets were subsequently wicked away from the edge of the grid with the filter paper strips (Whatman 541). The

grid was then rinsed three times with droplets of double distilled water each time removing the excess. Immediately after the last rinse, the grid was exposed to the staining solutions (1% uranyl formate) for 60 s and the stain was carefully removed using a fresh piece of filter paper. Finally, the grid was dried at ambient conditions for 2 h and used for TEM analysis. Empty AAV particles can be discerned by their ring-like shape from full particles, and both were manually counted.

Lentivirus generation

Packaging cells for LV production is described elsewhere.[42] Cells were transfected in 200 mL culture at 1×10^6 cells/mL cell density. Final DNA concentration of LV backbone plasmid in culture used for production was 0.4 μg/mL and DNA/PEI ratio 1:2. Transfection mixture was prepared in 5% of total cell culture volume with incubation time of 10–15 min. Production incubation conditions were 37°C, 120 rpm, and atmosphere with 5% CO_2. Four hours post transfection inducers cumate and coumermycin were added to final concentrations of 80 μg/mL and 10 nM, respectively. Sixteen hours post transfection sodium butyrate was added to a final concentration of 7 mM. Seventy-two hours post transfection cell culture was centrifuged at 300 × *g*, 5 min at 4°C, and supernatant containing LVs was filtered through a 0.45-μm membrane filter. Concentration was performed by ultracentrifugation on a sucrose cushion where 25% sucrose in 20 mM Tris-HCl, pH 7.5, is underlaid below the filtered lysate. Centrifugation was performed at 15,000 rpm for 3 h and 4°C on Beckman Optima L-80 XP ultracentrifuge with Type-19 fixed angle rotor (cat#325620). Pellet was resuspended in cell culture medium, aliquoted and stored at −80°C.

Functional LV titration by qPCR

HEK293A cells were plated in 96-well plates (25 000 cells/well) 4 h before transduction with LV. Samples of LV were prepared in 40x, 160x, 640x, 2560x dilutions in media containing 8 μg/mL polybrene and incubated at 37°C. Media was removed from the plated cells and 60 μL of LV dilution was added; 140 μL of fresh media is added 24 h after transduction. Transduced cells were kept in culture for 14 days and passed into a new plate when confluent. Genomic DNA of transduced cells was isolated with Qiagen blood and tissue kit. qPCR reaction was performed in 20 μL total volume containing 10 μL PrimeTime Gene Expression Master Mix (IDT cat#1055771), 0.6 μL primer/probe mix for target amplification 300 nM/150 nM final concentration, respectively, 0.6 μL primer/probe mix for reference gene (hALB) amplification 300 nM/150 nM final concentration, respectively, 4.8 μL nuclease-free H_2O, 4 μL of sample, standard or nuclease-free H_2O. For LV backbone amplification, primers LV-F (5′-TGAAAGCGAAAGGGAAACCAG-3′) and LV-R (5′-CACC CATCTCTCTCCTTCTAGCC-3′) were used with FAM probe LV-Pr (5′-6FAM-AGCTCTCTCGACGCAGGACTCGGC–BHQ1-3′). For reference gene amplification, primers hALB-F (5′-GCTGTCAT CTCTTGTGGGCTGT-3′) and hALB-R (5′-ACTCATGGGAGCT GCTGGTTC-3′) were used with HEX probe hALB-Pr (5′-6HEX-CCTGTCATGCCCACACAAATCTCTCC-BHQ1-3′). Standard curve was generated for each qPCR run with serial dilutions of standard from 10^8–10^2 copies per reaction. The following PCR conditions were used: initial denaturation (95°C, 3 min), 40 cycles of denaturation (95°C, 15 s) and annealing/extension (60°C, 1 min). The reaction was performed in a Quantstudio 5 qPCR instrument (Thermo Fisher Scientific), and analysis was performed in Quantstudio design and analysis software.

Transduction units were calculated using the following formula:

$$Titer\left[\frac{TU}{mL}\right] = \frac{n[cells] * X\left[\frac{copies}{cell}\right]}{V\,[mL]},$$

where n represents the number of transduced cells, X the integrated copies of LV per cell, and V the volume used for qPCR reaction in mL.

X is calculated using the following formula using the data obtained from qPCR:

$$X\left[\frac{copies}{cell}\right] = \frac{Copies\ of\ LV}{Copies\ of\ hALB} * 2.$$

Iodixanol step gradient ultracentrifugation

rAAV samples were purified using iodixanol step gradient ultracentrifugation adapted from Zolotukhin et al.[76] Twelve milliliters of sample was purified by underlaying 15 (5 mL), 25 (5 mL), 40 (7 mL), and 54% (5 mL) step gradients of iodixanol solution. To avoid rAAV aggregation, 15% iodixanol solution contained 1M NaCl. Centrifugation was performed at 385,000 × *g* for 1 h and 45 min in Beckman Optima L-80 XP ultracentrifuge with swinging bucket rotor. After centrifugation, 6.5 mL was taken with a syringe and needle 2 mm below the 40%/54% interface marked before starting the ultracentrifuge.

Flow cytometry

Emitted GFP fluorescence from 10,000 single cells per condition was acquired on a BD LSRFortessa (BD Biosciences, San Jose, CA) equipped with a 488-nm 100 mW laser and 530/30 bandpass filter. The population gating was performed on the parental cell line HEK293SF or 293SF-CymR/λR-GyrB. The fluorescence index was calculated by multiplying the percentage of GFP positive cells and the FITC mean fluorescence. The data were analyzed using BD FACSDiva software version 9.0.

Statistical analysis

For Figures 2, 4, and 7, one-way ANOVA with Tukey's multiple comparison test was performed. In Figure 3 A, Student's t test was performed for comparison of means. For Figure 5A, one-way ANOVA with Tukey's multiple comparison test was performed for Rep68 data, and Kruskal-Wallis test with Dunn's multiple comparison test was performed for Rep40 data due to D19 dataset not passing the normality test. For Table S4, one-way ANOVA with Tukey's multiple comparison test was performed for C8 Rep68, C24, and D19 data.

Kruskal-Wallis test with Dunn's multiple comparison test was performed for C8 Rep40 data due to dataset not passing the normality test. The difference between means was considered significant if $p < 0.05$.

DATA AND CODE AVAILABILITY

The authors confirm that the data supporting the findings of this study are available within the article (and/or) its supplementary materials.

SUPPLEMENTAL INFORMATION

Supplemental information can be found online at https://doi.org/10.1016/j.omtm.2023.07.002.

ACKNOWLEDGMENTS

This work was supported by funding from the National Research Council Canada, by the Québec Cell, Tissue and Gene Therapy Network –ThéCell (a thematic network supported by the Fonds de Recherche du Québec - Santé) and by the Natural Sciences and Engineering Research Council of Canada (stipend allocated to Lovro Jalšić via the NSERC-CREATE PrEEmiuM program). We would like to thank the expert technical assistance of Nazila Nazemi-Moghaddam, Sophie Broussau, and Nathalie Coulombe.

AUTHOR CONTRIBUTIONS

Investigation, L.J., V.L., S.M.E., S.H., N.N.; Conceptualization, L.J., P.S.C., B.G., R.G; Supervision, P.S.C., B.G., R.G.; Writing - original draft, L.J.; Writing-Review & Editing, L.J., P.S.C., B.G., R.G.; Funding acquisition, B.G., R.G.

DECLARATION OF INTERESTS

V.L. and R.G. are inventors on a patent application filed by the National Research Council Canada related to the cumate and coumermycin gene induction system and may receive royalty payments.

REFERENCES

1. Keeler, A.M., and Flotte, T.R. (2019). Recombinant Adeno-Associated Virus Gene Therapy in Light of Luxturna (and Zolgensma and Glybera): Where Are We, and How Did We Get Here? Annu. Rev. Virol. *6*, 601–621. https://doi.org/10.1146/annurev-virology-092818-015530.

2. Kotterman, M.A., and Schaffer, D.V. (2014). Engineering adeno-associated viruses for clinical gene therapy. Nat. Rev. Genet. *15*, 445–451. https://doi.org/10.1038/nrg3742.

3. Balakrishnan, B., and Jayandharan, G.R. (2014). Basic biology of adeno-associated virus (AAV) vectors used in gene therapy. Curr. Gene Ther. *14*, 86–100. http://www.ncbi.nlm.nih.gov/pubmed/24588706.

4. Mendelson, E., Trempe, J.P., and Carter, B.J. (1986). Identification of the trans-acting Rep proteins of adeno-associated virus by antibodies to a synthetic oligopeptide. J. Virol. *60*, 823–832. https://doi.org/10.1128/JVI.60.3.823-832.1986.

5. Tratschin, J.D., Miller, I.L., and Carter, B.J. (1984). Genetic analysis of adeno-associated virus: properties of deletion mutants constructed in vitro and evidence for an adeno-associated virus replication function. J. Virol. *51*, 611–619. http://www.ncbi.nlm.nih.gov/pubmed/6088786.

6. Green, M.R., and Roeder, R.G. (1980). Transcripts of the adeno-associated virus genome: mapping of the major RNAs. J. Virol. *36*, 79–92. https://doi.org/10.1128/JVI.36.1.79-92.1980.

7. Lusby, E.W., and Berns, K.I. (1982). Mapping of the 5' termini of two adeno-associated virus 2 RNAs in the left half of the genome. J. Virol. *41*, 518–526. https://doi.org/10.1128/JVI.41.2.518-526.1982.

8. Srivastava, A., Lusby, E.W., and Berns, K.I. (1983). Nucleotide sequence and organization of the adeno-associated virus 2 genome. J. Virol. *45*, 555–564. http://www.ncbi.nlm.nih.gov/pubmed/6300419%0Ahttp://www.pubmedcentral.nih.gov/articlerender.fcgi?artid=PMC256449.

9. Louis, N., Evelegh, C., and Graham, F.L. (1997). Cloning and sequencing of the cellular-viral junctions from the human adenovirus type 5 transformed 293 cell line. Virology *233*, 423–429. https://doi.org/10.1006/viro.1997.8597.

10. Dobrowsky, T., Gianni, D., Pieracci, J., and Suh, J. (2021). AAV manufacturing for clinical use: Insights on current challenges from the upstream process perspective. Curr. Opin. Biomed. Eng. *20*, 100353. https://doi.org/10.1016/j.cobme.2021.100353.

11. Saudan, P., Vlach, J., and Beard, P. (2000). Inhibition of S-phase progression by adeno-associated virus Rep78 protein is mediated by hypophosphorylated pRb. EMBO J. *19*, 4351–4361. https://doi.org/10.1093/emboj/19.16.4351.

12. Berthet, C., Raj, K., Saudan, P., and Beard, P. (2005). How adeno-associated virus Rep78 protein arrests cells completely in S phase. Proc. Natl. Acad. Sci. USA *102*, 13634–13639. https://doi.org/10.1073/pnas.0504583102.

13. Rommelaere, J., and Cornelis, J.J. (1991). Antineoplastic activity of parvoviruses. J. Virol. Methods *33*, 233–251. https://doi.org/10.1016/0166-0934(91)90024-t.

14. Winocour, E., Callaham, M.F., and Huberman, E. (1988). Perturbation of the cell cycle by adeno-associated virus. Virology *167*, 393–399. https://doi.org/10.1016/0042-6822(88)90100-6.

15. Qiao, C., Li, J., Skold, A., Zhang, X., and Xiao, X. (2002). Feasibility of generating adeno-associated virus packaging cell lines containing inducible adenovirus helper genes. J. Virol. *76*, 1904–1913. https://doi.org/10.1128/jvi.76.4.1904-1913.2002.

16. Hermanns, J., Schulze, A., Jansen-Db1urr, P., Kleinschmidt, J.A., Schmidt, R., and zur Hausen, H. (1997). Infection of primary cells by adeno-associated virus type 2 results in a modulation of cell cycle-regulating proteins. J. Virol. *71*, 6020–6027. https://doi.org/10.1128/JVI.71.8.6020-6027.1997.

17. Clark, K.R., Voulgaropoulou, F., Fraley, D.M., and Johnson, P.R. (1995). Cell lines for the production of recombinant adeno-associated virus. Hum. Gene Ther. *6*, 1329–1341. https://doi.org/10.1089/hum.1995.6.10-1329.

18. Gao, G.P., Qu, G., Faust, L.Z., Engdahl, R.K., Xiao, W., Hughes, J.V., Zoltick, P.W., and Wilson, J.M. (1998). High-titer adeno-associated viral vectors from a Rep/Cap cell line and hybrid shuttle virus. Hum. Gene Ther. *9*, 2353–2362. https://doi.org/10.1089/hum.1998.9.16-2353.

19. Chadeuf, G., Favre, D., Tessier, J., Provost, N., Nony, P., Kleinschmidt, J., Moullier, P., and Salvetti, A. (2000). Efficient recombinant adeno-associated virus production by a stable rep-cap HeLa cell line correlates with adenovirus-induced amplification of the integrated rep-cap genome. J. Gene Med. *2*, 260–268. https://doi.org/10.1002/1521-2254(200007/08)2:4<260::AID-JGM111>3.0.CO;2-8.

20. Mathews, L.C., Gray, J.T., Gallagher, M.R., and Snyder, R.O. (2002). Recombinant adeno-associated viral vector production using stable packaging and producer cell lines. Methods Enzymol. *346*, 393–413. https://doi.org/10.1016/s0076-6879(02)46068-5.

21. Martin, J., Frederick, A., Luo, Y., Jackson, R., Joubert, M., Sol, B., Poulin, F., Pastor, E., Armentano, D., Wadsworth, S., and Vincent, K. (2013). Generation and characterization of adeno-associated virus producer cell lines for research and preclinical vector production. Hum. Gene Ther. Methods *24*, 253–269. https://doi.org/10.1089/hgtb.2013.046.

22. Tamayose, K., Hirai, Y., and Shimada, T. (1996). A new strategy for large-scale preparation of high-titer recombinant adeno-associated virus vectors by using packaging cell lines and sulfonated cellulose column chromatography. Hum. Gene Ther. *7*, 507–513. https://doi.org/10.1089/hum.1996.7.4-507.

23. Inoue, N., and Russell, D.W. (1998). Packaging Cells Based on Inducible Gene Amplification for the Production of Adeno-Associated Virus Vectors. J. Virol. *72*, 7024–7031. https://doi.org/10.1128/jvi.72.9.7024-7031.1998.

24. Cao, L., During, M., and Xiao, W. (2002). Replication competent helper functions for recombinant AAV vector generation. Gene Ther. *9*, 1199–1206. https://doi.org/10.1038/sj.gt.3301710.

25. Gao, G.p., Lu, F., Sanmiguel, J.C., Tran, P.T., Abbas, Z., Lynd, K.S., Marsh, J., Spinner, N.B., and Wilson, J.M. (2002). Rep/Cap gene amplification and high-yield production of AAV in an A549 cell line expressing Rep/Cap. Mol. Ther. *5*, 644–649. https://doi.org/10.1006/mthe.2001.0591.

26. Farson, D., Harding, T.C., Tao, L., Liu, J., Powell, S., Vimal, V., Yendluri, S., Koprivnikar, K., Ho, K., Twitty, C., et al. (2004). Development and characterization of a cell line for large-scale, serum-free production of recombinant adeno-associated viral vectors. J. Gene Med. *6*, 1369–1381. https://doi.org/10.1002/jgm.622.

27. Qiao, C., Wang, B., Zhu, X., Li, J., and Xiao, X. (2002). A novel gene expression control system and its use in stable, high-titer 293 cell-based adeno-associated virus packaging cell lines. J. Virol. *76*, 13015–13027. https://doi.org/10.1128/jvi.76.24.13015-13027.2002.

28. Yuan, Z., Qiao, C., Hu, P., Li, J., and Xiao, X. (2011). A versatile adeno-associated virus vector producer cell line method for scalable vector production of different serotypes. Hum. Gene Ther. *22*, 613–624. https://doi.org/10.1089/hum.2010.241.

29. Mizukami, H., Okada, T., Ogasawara, Y., Matsushita, T., Urabe, M., Kume, A., and Ozawa, K. (2004). Separate control of Rep and Cap expression using mutant and wild-type loxP sequences and improved packaging system for adeno-associated virus vector production. Mol. Biotechnol. *27*, 7–14. https://doi.org/10.1385/MB:27:1:07.

30. Nakamura, S., Nakamura, R., Shibata, K., Kobayashi, M., Sahara, N., Shigeno, K., Shinjo, K., Naito, K., Ohnishi, K., Kasahara, N., and Iwaki, Y. (2004). Development of packaging cell lines for generation of adeno-associated virus vectors by lentiviral gene transfer of trans-complementary components. Eur. J. Haematol. *73*, 285–294. https://doi.org/10.1111/j.1600-0609.2004.00290.x.

31. Tratschin, J.D., Tal, J., and Carter, B.J. (1986). Negative and positive regulation in trans of gene expression from adeno-associated virus vectors in mammalian cells by a viral rep gene product. Mol. Cell Biol. *6*, 2884–2894. https://doi.org/10.1128/mcb.6.8.2884.

32. Beaton, A., Palumbo, P., and Berns, K.I. (1989). Expression from the adeno-associated virus p5 and p19 promoters is negatively regulated in trans by the rep protein. J. Virol. *63*, 4450–4454. https://doi.org/10.1128/jvi.63.10.4450-4454.1989.

33. Kyöstiö, S.R., Wonderling, R.S., and Owens, R.A. (1995). Negative regulation of the adeno-associated virus (AAV) P5 promoter involves both the P5 rep binding site and the consensus ATP-binding motif of the AAV Rep68 protein. J. Virol. *69*, 6787–6796. https://doi.org/10.1128/jvi.69.11.6787-6796.1995.

34. Labow, M.A., Hermonat, P.L., and Berns, K.I. (1986). Positive and negative autoregulation of the adeno-associated virus type 2 genome. J. Virol. *60*, 251–258. https://doi.org/10.1128/jvi.60.1.251-258.1986.

35. Thorne, B.A., Takeya, R.K., and Peluso, R.W. (2009). Manufacturing recombinant adeno-associated viral vectors from producer cell clones. Hum. Gene Ther. *20*, 707–714. https://doi.org/10.1089/hum.2009.070.

36. Dumont, J., Euwart, D., Mei, B., Estes, S., and Kshirsagar, R. (2016). Human cell lines for biopharmaceutical manufacturing: history, status, and future perspectives. Crit. Rev. Biotechnol. *36*, 1110–1122. https://doi.org/10.3109/07388551.2015.1084266.

37. Tan, E., Chin, C.S.H., Lim, Z.F.S., and Ng, S.K. (2021). HEK293 Cell Line as a Platform to Produce Recombinant Proteins and Viral Vectors. Front. Bioeng. Biotechnol. *9*, 796991. https://doi.org/10.3389/fbioe.2021.796991.

38. Chang, L.S., Shi, Y., and Shenk, T. (1989). Adeno-associated virus P5 promoter contains an adenovirus E1A-inducible element and a binding site for the major late transcription factor. J. Virol. *63*, 3479–3488. http://www.ncbi.nlm.nih.gov/pubmed/2545917%0Ahttp://www.pubmedcentral.nih.gov/articlerender.fcgi?artid=PMC250925.

39. Yang, Q., Chen, F., and Trempe, J.P. (1994). Characterization of cell lines that inducibly express the adeno-associated virus Rep proteins. J. Virol. *68*, 4847–4856. https://doi.org/10.1128/JVI.68.8.4847-4856.1994.

40. Mullick, A., Xu, Y., Warren, R., Koutroumanis, M., Guilbault, C., Broussau, S., Malenfant, F., Bourget, L., Lamoureux, L., Lo, R., et al. (2006). The cumate gene-switch: a system for regulated expression in mammalian cells. BMC Biotechnol. *6*, 43. https://doi.org/10.1186/1472-6750-6-43.

41. Zhao, H.F., Boyd, J., Jolicoeur, N., and Shen, S.H. (2003). A coumermycin/novobiocin-regulated gene expression system. Hum. Gene Ther. *14*, 1619–1629. https://doi.org/10.1089/104303403322542266.

42. Broussau, S., Lytvyn, V., Simoneau, M., Guilbault, C., Leclerc, M., Nazemi-Moghaddam, N., Coulombe, N., Elahi, S.M., McComb, S., and Gilbert, R. (2023). Packaging cells for lentiviral vectors generated using the cumate and coumermycin gene induction systems and nanowell single-cell cloning. Mol. Ther. Methods Clin. Dev. *29*, 40–57. https://doi.org/10.1016/j.omtm.2023.02.013.

43. Seyffert, M., Glauser, D.L., Schraner, E.M., de Oliveira, A.P., Mansilla-Soto, J., Vogt, B., Büning, H., Linden, R.M., Ackermann, M., and Fraefel, C. (2017). Novel Mutant AAV2 Rep Proteins Support AAV2 Replication without Blocking HSV-1 Helpervirus Replication. PLoS One *12*, e0170908. https://doi.org/10.1371/journal.pone.0170908.

44. Prasad, K.M., Zhou, C., and Trempe, J.P. (1997). Characterization of the Rep78/adeno-associated virus complex. Virology *229*, 183–192. https://doi.org/10.1006/viro.1996.8431.

45. Davis, M.D., Wu, J., and Owens, R.A. (2000). Mutational analysis of adeno-associated virus type 2 Rep68 protein endonuclease activity on partially single-stranded substrates. J. Virol. *74*, 2936–2942. https://doi.org/10.1128/jvi.74.6.2936-2942.2000.

46. Hickman, A.B., Ronning, D.R., Perez, Z.N., Kotin, R.M., and Dyda, F. (2004). The Nuclease Domain of Adeno-Associated Virus Rep Coordinates Replication Initiation Using Two Distinct DNA Recognition Interfaces. Mol. Cell. *13*, 403–414. https://doi.org/10.1016/S1097-2765(04)00023-1.

47. Urabe, M., Hasumi, Y., Kume, A., Surosky, R.T., Kurtzman, G.J., Tobita, K., and Ozawa, K. (1999). Charged-to-alanine scanning mutagenesis of the N-terminal half of adeno-associated virus type 2 Rep78 protein. J. Virol. *73*, 2682–2693. https://doi.org/10.1128/jvi.73.4.2682-2693.1999.

48. Smith, R.H., and Kotin, R.M. (2000). An adeno-associated virus (AAV) initiator protein, Rep78, catalyzes the cleavage and ligation of single-stranded AAV ori DNA. J. Virol. *74*, 3122–3129. https://doi.org/10.1128/jvi.74.7.3122-3129.2000.

49. Snyder, R.O., Im, D.S., Ni, T., Xiao, X., Samulski, R.J., and Muzyczka, N. (1993). Features of the adeno-associated virus origin involved in substrate recognition by the viral Rep protein. J. Virol. *67*, 6096–6104. https://doi.org/10.1128/jvi.67.10.6096-6104.1993.

50. Young, S.M., McCarty, D.M., Degtyareva, N., and Samulski, R.J. (2000). Roles of Adeno-Associated Virus Rep Protein and Human Chromosome 19 in Site-Specific Recombination. J. Virol. *74*, 3953–3966. https://doi.org/10.1128/JVI.74.9.3953-3966.2000.

51. Im, D.S., and Muzyczka, N. (1990). The AAV origin binding protein Rep68 is an ATP-dependent site-specific endonuclease with DNA helicase activity. Cell *61*, 447–457. https://doi.org/10.1016/0092-8674(90)90526-k.

52. King, J.A., Dubielzig, R., Grimm, D., and Kleinschmidt, J.A. (2001). DNA helicase-mediated packaging of adeno-associated virus type 2 genomes into preformed capsids. EMBO J. *20*, 3282–3291. https://doi.org/10.1093/emboj/20.12.3282.

53. Li, Z., Brister, J.R., Im, D.S., and Muzyczka, N. (2003). Characterization of the adenoassociated virus Rep protein complex formed on the viral origin of DNA replication. Virology *313*, 364–376. https://doi.org/10.1016/s0042-6822(03)00340-4.

54. Iyer, L.M., Makarova, K.S., Koonin, E.V., and Aravind, L. (2004). Comparative genomics of the FtsK-HerA superfamily of pumping ATPases: implications for the origins of chromosome segregation, cell division and viral capsid packaging. Nucleic Acids Res. *32*, 5260–5279. https://doi.org/10.1093/nar/gkh828.

55. James, J.A., Aggarwal, A.K., Linden, R.M., and Escalante, C.R. (2004). Structure of adeno-associated virus type 2 Rep40-ADP complex: insight into nucleotide recognition and catalysis by superfamily 3 helicases. Proc. Natl. Acad. Sci. USA *101*, 12455–12460. https://doi.org/10.1073/pnas.0403454101.

56. Yoon-Robarts, M., Blouin, A.G., Bleker, S., Kleinschmidt, J.A., Aggarwal, A.K., Escalante, C.R., and Linden, R.M. (2004). Residues within the B' motif are critical for DNA binding by the superfamily 3 helicase Rep40 of adeno-associated virus type 2. J. Biol. Chem. *279*, 50472–50481. https://doi.org/10.1074/jbc.M403900200.

57. Zarate-Perez, F., Bardelli, M., Burgner, J.W., Villamil-Jarauta, M., Das, K., Kekilli, D., Mansilla-Soto, J., Linden, R.M., and Escalante, C.R. (2012). The interdomain linker of AAV-2 Rep68 is an integral part of its oligomerization domain: role of a conserved SF3 helicase residue in oligomerization. PLoS Pathog. *8*, e1002764. https://doi.org/10.1371/journal.ppat.1002764.

58. Zarate-Perez, F., Mansilla-Soto, J., Bardelli, M., Burgner, J.W., Villamil-Jarauta, M., Kekilli, D., Samso, M., Linden, R.M., and Escalante, C.R. (2013). Oligomeric

properties of adeno-associated virus Rep68 reflect its multifunctionality. J. Virol. *87*, 1232–1241. https://doi.org/10.1128/JVI.02441-12.

59. Hörer, M., Weger, S., Butz, K., Hoppe-Seyler, F., Geisen, C., and Kleinschmidt, J.A. (1995). Mutational analysis of adeno-associated virus Rep protein-mediated inhibition of heterologous and homologous promoters. J. Virol. *69*, 5485–5496. http://www.ncbi.nlm.nih.gov/pubmed/7636994.

60. Di Pasquale, G., and Chiorini, J.A. (2003). PKA/PrKX activity is a modulator of AAV/adenovirus interaction. EMBO J. *22*, 1716–1724. https://doi.org/10.1093/emboj/cdg153.

61. Chiorini, J.A., Zimmermann, B., Yang, L., Smith, R.H., Ahearn, A., Herberg, F., and Kotin, R.M. (1998). Inhibition of PrKX, a novel protein kinase, and the cyclic AMP-dependent protein kinase PKA by the regulatory proteins of adeno-associated virus type 2. Mol. Cell Biol. *18*, 5921–5929. https://doi.org/10.1128/mcb.18.10.5921.

62. Li, J., Samulski, R.J., and Xiao, X. (1997). Role for highly regulated rep gene expression in adeno-associated virus vector production. J. Virol. *71*, 5236–5243. https://doi.org/10.1128/JVI.71.7.5236-5243.1997.

63. Hölscher, C., Kleinschmidt, J.A., and Bürkle, A. (1995). High-level expression of adeno-associated virus (AAV) Rep78 or Rep68 protein is sufficient for infectious-particle formation by a rep-negative AAV mutant. J. Virol. *69*, 6880–6885. https://doi.org/10.1128/JVI.69.11.6880-6885.1995.

64. Chejanovsky, N., and Carter, B.J. (1989). Mutagenesis of an AUG codon in the adeno-associated virus rep gene: effects on viral DNA replication. Virology *173*, 120–128. https://doi.org/10.1016/0042-6822(89)90227-4.

65. Ede, C., Chen, X., Lin, M.Y., and Chen, Y.Y. (2016). Quantitative Analyses of Core Promoters Enable Precise Engineering of Regulated Gene Expression in Mammalian Cells. ACS Synth. Biol. *5*, 395–404. https://doi.org/10.1021/acssynbio.5b00266.

66. Grimm, D., Lee, J.S., Wang, L., Desai, T., Akache, B., Storm, T.A., and Kay, M.A. (2008). In Vitro and In Vivo Gene Therapy Vector Evolution via Multispecies Interbreeding and Retargeting of Adeno-Associated Viruses. J. Virol. *82*, 5887–5911. https://doi.org/10.1128/JVI.00254-08.

67. Demeulemeester, J., De Rijck, J., Gijsbers, R., and Debyser, Z. (2015). Retroviral integration: Site matters: Mechanisms and consequences of retroviral integration site selection. Bioessays *37*, 1202–1214. https://doi.org/10.1002/bies.201500051.

68. Chahal, P.S., Schulze, E., Tran, R., Montes, J., and Kamen, A.A. (2014). Production of adeno-associated virus (AAV) serotypes by transient transfection of HEK293 cell suspension cultures for gene delivery. J. Virol. Methods *196*, 163–173. https://doi.org/10.1016/j.jviromet.2013.10.038.

69. Côté, J., Garnier, A., Massie, B., and Kamen, A. (1998). Serum-free production of recombinant proteins and adenoviral vectors by 293SF-3F6 cells. Biotechnol. Bioeng. *59*, 567–575. http://www.ncbi.nlm.nih.gov/pubmed/10099373.

70. Broussau, S., Jabbour, N., Lachapelle, G., Durocher, Y., Tom, R., Transfiguracion, J., Gilbert, R., and Massie, B. (2008). Inducible Packaging Cells for Large-scale Production of Lentiviral Vectors in Serum-free Suspension Culture. Mol. Ther. *16*, 500–507. https://doi.org/10.1038/sj.mt.6300383.

71. Gervais, C., Paquette, D., Burns-Tardif, A., Martin, L., and Massie, B. (1998). Development of High Output Expression Vectors for Antibody Production in Mammalian Cells. In Animal Cell Technology: Basic & Applied Aspects (Springer Netherlands), pp. 349–354. https://doi.org/10.1007/978-94-011-5161-0_60.

72. Durocher, Y., Perret, S., and Kamen, A. (2002). High-level and high-throughput recombinant protein production by transient transfection of suspension-growing human 293-EBNA1 cells. Nucleic Acids Res. *30*, E9. https://doi.org/10.1093/nar/30.2.e9.

73. Cheng, L., Du, C., Murray, D., Tong, X., Zhang, Y.A., Chen, B.P., and Hawley, R.G. (1997). A GFP reporter system to assess gene transfer and expression in human hematopoietic progenitor cells. Gene Ther. *4*, 1013–1022. https://doi.org/10.1038/sj.gt.3300507.

74. Aurnhammer, C., Haase, M., Muether, N., Hausl, M., Rauschhuber, C., Huber, I., Nitschko, H., Busch, U., Sing, A., Ehrhardt, A., and Baiker, A. (2012). Universal Real-Time PCR for the Detection and Quantification of Adeno-Associated Virus Serotype 2-Derived Inverted Terminal Repeat Sequences. Hum. Gene Ther. Methods *23*, 18–28. https://doi.org/10.1089/hgtb.2011.034.

75. Lin, Y.C., Boone, M., Meuris, L., Lemmens, I., Van Roy, N., Soete, A., Reumers, J., Moisse, M., Plaisance, S., Drmanac, R., et al. (2014). Genome dynamics of the human embryonic kidney 293 lineage in response to cell biology manipulations. Nat. Commun. *5*, 4767. https://doi.org/10.1038/ncomms5767.

76. Zolotukhin, S., Byrne, B.J., Mason, E., Zolotukhin, I., Potter, M., Chesnut, K., Summerford, C., Samulski, R.J., and Muzyczka, N. (1999). Recombinant adeno-associated virus purification using novel methods improves infectious titer and yield. Gene Ther. *6*, 973–985. https://doi.org/10.1038/sj.gt.3300938.